NOAA Technical Report NESS 71

An Intercomparison of Meteorological Parameters Derived From Radiosonde and Satellite Vertical Temperature Cross Sections

W. L. SMITH AND H. M. WOOLF

WASHINGTON, D.C.
NOVEMBER 1974

noaa NATIONAL OCEANIC AND ATMOSPHERIC ADMINISTRATION / National Environmental Satellite Service

National Environmental Satellite Service Series

The National Environmental Satellite Service (NESS) is responsible for the establishment and operation of the environmental satellite systems of NOAA.

Publication of a report in NOAA Technical Report NESS series will not preclude later publication in an expanded or modified form in scientific journals. NESS series of NOAA Technical Reports is a continuation of, and retains the consecutive numbering sequence of, the former series, ESSA Technical Report National Environmental Satellite Center (NESC), and of the earlier series, Weather Bureau Meteorological Satellite Laboratory (MSL) Report. Reports 1 through 37 are listed in publication NESC 56 of this series.

Reports 1 through 50 in the series are available from the National Technical Information Service (NTIS), U.S. Department of Commerce, Sills Bldg., 5285 Port Royal Road, Springfield, Va. 22151, in paper copy or microfiche form. Order by accession number, when given, in parentheses. Beginning with 51, printed copies of the reports are available through the Superintendent of Documents, U.S. Government Printing Office, Washington, D.C. 20402; microfiche available from NTIS (use accession number when available). Prices given on request from the Superintendent of Documents or NTIS.

ESSA Technical Reports

NESC 38 Angular Distribution of Solar Radiation Reflected From Clouds as Determined From TIROS IV Radiometer Measurements. I. Ruff, R. Koffler, S. Fritz, J. S. Winston, and P. K. Rao, March 1967. (PB-174-729)

NESC 39 Motions in the Upper Troposphere as Revealed by Satellite Observed Cirrus Formations. H. McClure Johnson, October 1966. (PB-173-996)

NESC 40 Cloud Measurements Using Aircraft Time-Lapse Photography. Linwood F. Whitney, Jr., and E. Paul McClain, April 1967. (PB-174-728)

NESC 41 The SINAP Problem: Present Status and Future Prospects; Proceedings of a Conference Held at the National Environmental Satellite Center, Suitland, Maryland, January 18-20, 1967. E. Paul McClain, October 1967. (PB-176-570)

NESC 42 Operational Processing of Low Resolution Infrared (LRIR) Data From ESSA Satellites. Louis Rubin, February 1968. (PB-178-123)

NESC 43 Atlas of World Maps of Long-Wave Radiation and Albedo--for Seasons and Months Based on Measurements From TIROS IV and TIROS VII. J. S. Winston and V. Ray Taylor, September 1967. (PB-176-569)

NESC 44 Processing and Display Experiments Using Digitized ATS-1 Spin Scan Camera Data. M. B. Whitney, R. C. Doolittle, and B. Goddard, April 1968. (PB-178-424)

NESC 45 The Nature of Intermediate-Scale Cloud Spirals. Linwood F. Whitney, Jr., and Leroy D. Herman, May 1968. (AD-673-681)

NESC 46 Monthly and Seasonal Mean Global Charts of Brightness From ESSA 3 and ESSA 5 Digitized Pictures, February 1967-February 1968. V. Ray Taylor and Jay S. Winston, November 1968. (PB-180-717)

NESC 47 A Polynomial Representation of Carbon Dioxide and Water Vapor Transmission. William L. Smith, February 1969. (PB-183-296)

NESC 48 Statistical Estimation of the Atmosphere's Geopotential Height Distribution From Satellite Radiation Measurements. William L. Smith, February 1969. (PB-183-297)

NESC 49 Synoptic/Dynamic Diagnosis of a Developing Low-Level Cyclone and Its Satellite-Viewed Cloud Patterns. Harold J. Brodrick and E. Paul McClain, May 1969. (PB-184-612)

NESC 50 Estimating Maximum Wind Speed of Tropical Storms From High Resolution Infrared Data. L. F. Hubert, A. Timchalk, and S. Fritz, May 1969. (PB-184-611)

(Continued on inside back cover)

NOAA Technical Report NESS 71

An Intercomparison of Meteorological Parameters Derived From Radiosonde and Satellite Vertical Temperature Cross Sections

W. L. SMITH AND H. M. WOOLF

WASHINGTON, D.C.
NOVEMBER 1974

UNITED STATES
DEPARTMENT OF COMMERCE
Frederick B. Dent, Secretary

NATIONAL OCEANIC AND
ATMOSPHERIC ADMINISTRATION
Robert M. White, Administrator

National Environmental
Satellite Service
David S. Johnson, Director

CONTENTS

Mention of a commercial company or product does not constitute an endorsement by the NOAA National Environmental Satellite Service. Use for publicity or advertising purposes of information from this publication concerning proprietary products or the tests of such products is not authorized.

For sale by the Superintendent of Documents, U.S. Government Printing Office, Washington, D.C., 20402. Price $0.65

AN INTERCOMPARISON OF METEOROLOGICAL PARAMETERS DERIVED FROM RADIOSONDE AND SATELLITE VERTICAL TEMPERATURE CROSS SECTIONS

W. L. Smith and H. M. Woolf
National Environmental Satellite Service, NOAA, Washington, D.C.

ABSTRACT. Vertical cross-sections of temperature between 60°S and 50°N for Apr. 6, 1973, are derived from (a) radiosonde, (b) Nimbus-5 Infrared Temperature Profile Radiometer, Nimbus-E Microwave Spectrometer and Selective Chopper Radiometer, and (c) NOAA-2 Vertical Temperature Profile Radiometer (VTPR) data. Comparisons are made of the level temperatures and latitudinal temperature gradients, geopotential heights and the latitudinal gradients, and geostrophic winds inferred from the radiosonde and satellite cross-sections. The results of this limited case study indicate:

1. Temperature accuracies for the lower troposphere obtained with Nimbus-5 sounding data are superior to those achieved with the NOAA-2 VTPR data.

2. The agreement between latitudinal gradients of temperature derived from satellite data and radiosonde observations is much better than the agreement between level temperatures obtained from satellite and radiosonde observations.

3. The geostrophic wind distribution of jet streams derived from satellite data possesses more character and intensity than does the geostrophic wind distribution obtained from radiosonde data.

I. INTRODUCTION

Comparisons are made of vertical cross-sections of radiosonde, Nimbus-5, and NOAA-2 temperature profiles that were observed at nearly the same time about a line extending from 60°S to 50°N on Apr. 6, 1973. Figure 1 shows the distribution of the radiosonde, Nimbus-5, and NOAA Vertical Temperature Profile Radiometer (VTPR) data analyzed.[1] The satellite profile observations selected were those that were geographically closest to the radiosonde stations. Since the VTPR was spatially scanning, better space coincidence with the radiosonde observations was

[1]All figures are grouped together at the back of the study.

achieved than with the suborbital track-restricted Nimbus-5 data.[2] The more uniform north-south distribution, however, of the Nimbus-5 data makes it more amenable to vertical cross-section analysis than the radiosonde or VTPR data.

Figure 2 shows the north-south distributions of cloudiness in percentages reaching various pressure levels, total precipitable water as derived from both the NEMS-microwave and the ITPR-infrared data, and total outgoing longwave flux (langleys/day) as derived from the Nimbus-5 radiance observations. Also shown is a pictorial image of the cloud distribution obtained from the 4 n.mi. resolution scanning THIR aboard Nimbus 5. Note in the THIR cloud photograph that there apparently are two jet streams (indicated by the cirrus streaks) crossing the Nimbus orbital track, a subtropical jet near 25°N and a merging polar front jet near 35°N. As will be shown, the existence of these jet streams is verified by the thermal winds derived from both the satellite and radiosonde data.

Before proceeding with a discussion of the results, it is important to point out certain general features of the Nimbus-5 and NOAA-2 satellite temperature profile retrievals (for details, see Smith et al. 1974 and McMillin et al. 1973).

1. The NOAA-2 VTPR retrieval method uses the 12-hr forecast as an initial guess. The temperature profile obtained using the "minimum information solution" (Fleming and Smith 1972) is the minimum perturbation of the initial profile required to satisfy the outgoing radiance observations. As a result, vertical structure in the 12-hr forecast below the vertical resolution of the radiance observations is retained in the satellite profile retrieval.

2. The Nimbus-5 [ITPR + NEMS + SCR (Selective Chopper Radiometer)] retrieval system utilizes regression equations relating temperature to radiances, generated from a climatological sample of radiosonde data, to obtain the initial profile used in the minimum information solution. Consequently, the Nimbus retrievals are independent of contemporary radiosonde or forecast information.

3. Figure 1 shows that the Nimbus-5, NOAA-VTPR, and RAOB data geographically are not entirely coincident. The most important systematic geographical discrepancy is north of 30°N where the Nimbus data are located over China and the VTPR and radiosonde data are located over Japan.

II. DISCUSSION OF RESULTS

Figures 3, 4, and 5 are cross sections of RAOB, Nimbus-5, and VTPR temperatures. Figures 6 and 7 show the difference of Nimbus-5 and VTPR retrievals with respect to the radiosonde observations. In the troposphere, differences with the radiosonde (RAOB) are generally small

[2]The Infrared Temperature Profile Radiometer (ITPR) on Nimbus 5 was designed with an east-west scan capability. Owing to a scan mechanism malfunction, however, the ITPR was stopped in the nadir-looking position during this orbit.

except around 25°N where +6°C (Nimbus-5) and +10°C (VTPR) differences occur. Looking at figure 1, however, we see that the RAOB location is 7° west of the Nimbus-5 and VTPR observations. In the tropopause region, 300 to 100 mb, large differences of Nimbus-5 and RAOB observations result from vertical resolution limitations of the satellite sensor. The VTPR-RAOB differences are smaller because of the good "first guess" used in the VTPR retrievals. This is verified by the differences, shown in figure 8, between the 12-hr forecast (used as the VTPR first guess) and the RAOB. Since the Nimbus-5 retrievals do not use such contemporary first-guess information, larger differences in the tropopause region are expected.

Note the vertical compensation of the errors. Probably, the most important feature illustrated in figures 6 and 7 is that the errors (or differences) are spatially correlated so that one would expect smaller differences between the spatial gradients than between the point values.

Figure 9 shows comparisons of the horizontal gradients, over 3° of latitude, at isobaric levels of temperatures derived from the RAOB and Nimbus-5 soundings. There is very good correspondence between the two fields of temperature gradients. The differences are probably within the noise level expected to exist between two RAOBs spaced 3° of latitude apart and those due to the different locations of the RAOB and the Nimbus-5 data.

Figure 10 shows comparisons of the geostrophic wind derived from the Nimbus-5 and RAOB temperature cross-sections. The overall agreement of the distribution of wind associated with the jet streams is quite good. This experimental result confirms the theoretical study presented by Togstad and Horn (1974). The different location of the wind maximum is probably a result of the different longitudinal orientation of the RAOB and Nimbus-5 data (see fig. 1). The fact that the Nimbus-5 pattern displays more character and stronger maximum winds is probably because of the higher density of Nimbus-5 soundings.

Figures 11 through 14 present various statistics obtained from the entire 60°S to 50°N cross-sections. Part (a) of each figure shows the standard deviations between the radiosonde profiles and those obtained from the dynamical forecast (i.e., the initial profile used in the VTPR solution), the VTPR soundings, and the Nimbus-5 soundings. Part (b) of each figure shows the correlation of the differences between the satellite soundings and the radiosonde observations with the differences between the forecast soundings and the radiosonde observations. Finally, part (c) shows the minimum standard deviation expected between the radiosonde observations and an analysis constructed by updating the forecast with the satellite soundings. This analysis procedure, initially suggested by Bonner (1974), consists of prescribing the analyzed temperature at each level as a linear combination of the forecast temperature and the satellite-derived temperature. The weighting coefficient of this linear equation is obtained through a minimization procedure. Its numerical value is a function of the expected standard errors of the forecast and the satellite retrieval, as well as the expected correlation of forecast and satellite profile errors. (In this analysis, the radiosonde observations are taken as "truth" in computing these statistically expected values.)

Since here the weighting coefficient has been defined in an optimum way, using "the radiosonde truth" for its determination, the final analysis result is bound to be more accurate than either the forecast or satellite value. Although an optimum weighting coefficient cannot be defined in practice (since "truth" is always unknown), this analysis procedure is still a convenient way of illustrating the added information content of the satellite soundings over that already contained in the dynamical forecast.

In figure 11(a), we see that, below the 500-mb level, the Nimbus data agree much better with the radiosonde data than do the VTPR observations. This result most likely is due to the superior ability of the Nimbus-5 sounders to probe into, between, and through clouds. (The Nimbus-5 ITPR has four times the area resolution of the NOAA-2 VTPR, and the Nimbus-5 NEMS microwave instrument is able to probe directly through clouds.) In the tropopause region, however, the Nimbus-5 soundings are inferior to the VTPR profiles. The superiority of the VTPR profiles probably is a result of the incorporation of the 12-hr forecast in the solution. Evidence of this is given in the correlation coefficient profiles in part (b). We see that, in the upper troposphere, the error of the VTPR retrieval is highly correlated with the error of the 12-hr forecast, indicating that the forecast has a dramatic influence on the VTPR profile result.

Note the high correlations of the error of the forecast-independent Nimbus-5 retrievals and the error of the forecast in the surface layer below 700 mb and in the 200- to 500-mb region. This apparently is due to the fact that both the forecast profiles and Nimbus-5 satellite profiles tend to smooth through fine-scale vertical structures such as surface and tropopause inversions. Consequently, since both the forecast and satellite retrievals resolve a similar vertical scale which is larger than that resolved by the radiosonde, a high correlation results in regions where fine-scale structure exists. The fact that the VTPR error is slightly less correlated than the Nimbus-5 error in the lower troposphere probably is a result of cloud noise.

Combining the satellite data with the 12-hr forecast using optimum weights yields the analysis result shown in figure 11(c). Note that the most dramatic influence of the satellite data is above the 700-mb level for both the Nimbus-5 and VTPR retrieval cases. The minor influence below 700 mb is a result of the relatively high error correlations (the vertical scale correlation discussed above) and the fact that the forecast profiles are relatively accurate. Remember, however, that the forecast probably is unrepresentatively accurate for this case since the cross-section area is within, and downstream of, a dense network of radiosonde data. Also note that the large differences between the Nimbus-5 and VTPR standard deviations with radiosondes are diminished greatly when the retrievals are combined with the 12-hr forecast using optimum weights to produce the analysis result. This result suggests that the differences between the two satellite profiles shown in figure 11(a) mainly are due to the differences in the initial profile used in the retrieval process and not to the information content of the radiance observations. The differences in information content of the two satellite sounding systems are reflected more accurately in figure 11(c).

Figures 12, 13, and 14 show similar statistical results for temperature gradients, geopotential heights, and geostrophic winds. In viewing the standard deviation portions (a) of each figure, we note that the satellite results are generally inferior to the relatively accurate 12 hr forecast results. Portion (c), however, of each figure reveals that the satellite data, when added to the forecast profiles to construct an analysis, leads to a significant reduction of the error of the forecast although that error is relatively small (in this case). Of course, one would expect to see an even more dramatic impact of the satellite data in situations where the forecast error is much larger, which is more likely to be the case in areas where radiosonde data are sparse.

III. CONCLUSIONS

This limited case study has revealed the following characteristics of the Nimbus-5 and VTPR temperature retrieval data:

1. Much better agreement exists between temperature gradients derived from Nimbus-5, VTPR, and radiosonde data than between the absolute temperatures. (Compare figs. 11 and 12.) This indicates that the satellite retrievals possess large horizontal scale bias errors that could be caused by (a) biases in the initial data used in the retrieval process (i.e., statistical or dynamical forecast data), (b) biases caused by aerosols or undetected large-scale cloudiness, or (c) systematic errors in the weighting functions.

2. The geostrophic wind distribution associated with intense baroclinic phenomena (e.g., the jet stream) can be diagnosed accurately from the satellite temperature retrieval data. The results shown here indicate that the Nimbus-5 results may even be superior to radiosonde results, suggesting that the thermal gradients obtained from the closely spaced Nimbus data are more accurate than those obtained from the more coarsely spaced radiosonde observations.

3. Even in regions where the forecast is relatively accurate, such as the case investigated here, the satellite retrieval data are sufficiently independent to provide an analysis with an accuracy superior to that of the forecast.

ACKNOWLEDGMENTS

The authors appreciate the contributions of L. Mannello and P. Pellegrino who plotted and analyzed the cross sections and prepared the data for computer processing.

REFERENCES

Bonner, William D. (National Meteorological Center, National Weather Service, U.S. Department of Commerce, Washington, D.C.), "An Analysis Procedure Constructed by Updating a Forecast With Satellite Soundings," 1974 (unpublished memorandum).

Fleming, H. E., and Smith, W. L., "Inversion Techniques for Remote Sensing of Atmospheric Temperature Profiles," Temperature, Its Measurement and Control in Science and Industry, Vol. 4, Part 3, Instrument Society of America, Pittsburgh, Pa., Apr. 1972, pp. 2239-2250.

McMillin, L. M., Wark, D. Q., Siomkajlo, J. M., Abel, P. G., Werbowetzki, A., Lauritson, L. A., Pritchard, J. A., Crosby, D. S., Woolf, H. M., Luebbe, R. C., Weinreb, M. P., Fleming, H. E., Bittner, F. E., and Hayden, C. M., "Satellite Infrared Soundings From NOAA Spacecraft," NOAA Technical Report NESS 65, National Environmental Satellite Service, National Oceanic and Atmospheric Administration, U.S. Department of Commerce, Washington, D.C., Sept. 1973, 108 pp.

Smith, W. L., Woolf, H. M., Abel, P. G., Hayden, C. M., Chalfant, M., and Grody, N., "Nimbus-5 Sounder Data Processing System; Part I: Measurement Characteristics and Data Reduction Procedures," NOAA Technical Memorandum NESS 57, National Environmental Satellite Service, National Oceanic and Atmospheric Administration, U.S. Department of Commerce, Washington, D.C., June 1974, 99 pp.

Togstad, William E., and Horn, Lyle H., "An Application of the Satellite Indirect Sounding Technique in Describing the Hyperbaroclinic Zone of a Jet Streak," Journal of Applied Meteorology, Vol. 13, No. 2, Mar. 1974, pp. 264-276.

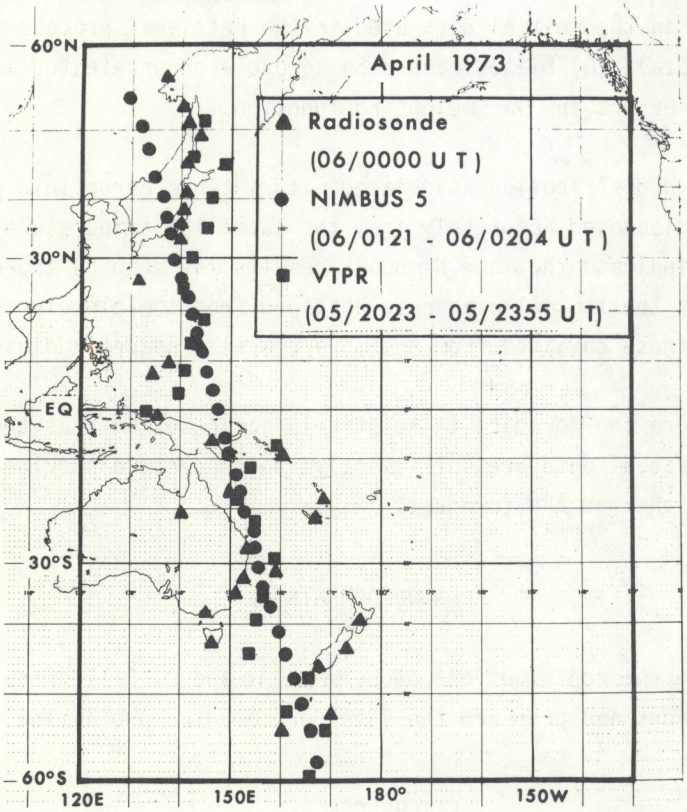

Figure 1.--Geographical locations of radiosonde, Nimbus-5, and NOAA VTPR soundings. UT, Universal Time, is equivalent to GMT, Greenwich Meridian Time.

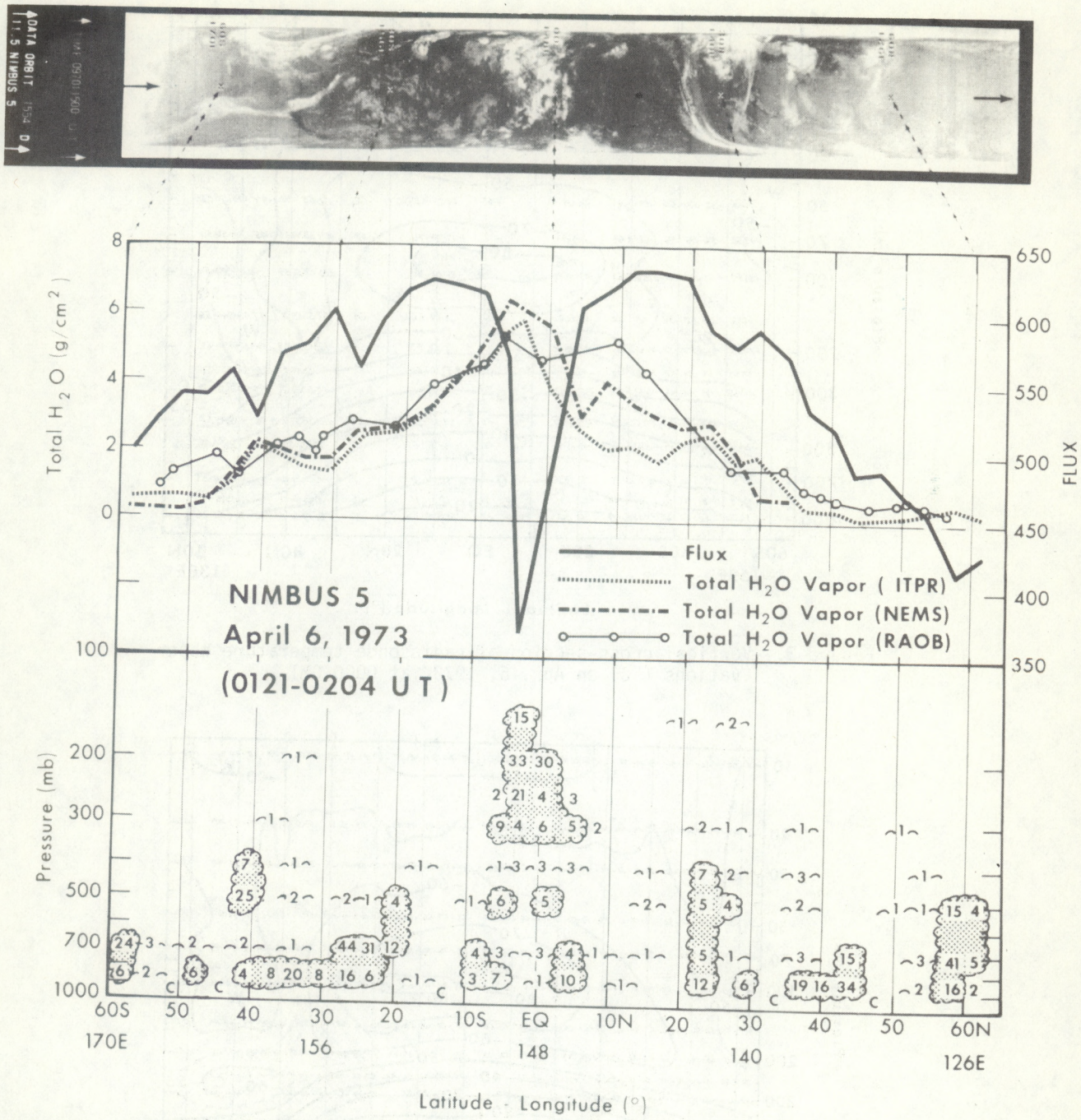

Figure 2.--Latitude cross-section of total integrated water vapor (g/cm^2), total outgoing longwave flux (langleys/day), amount (%) of cloudiness reaching various pressure levels (derived from the Nimbus-5 radiance measurements). The cloud image obtained from the Nimbus-5 Temperature Humidity Infrared Radiometer (THIR) appears at the top. NEMS represents Nimbus-E Microwave Spectrometer, and RAOB represents Radiosonde Observation.

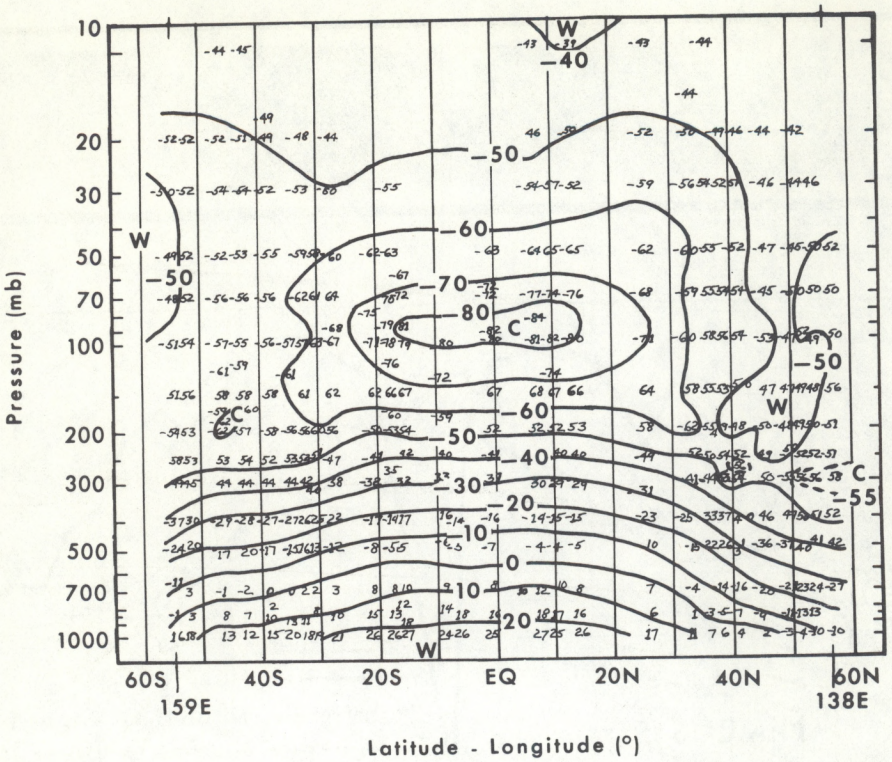

Figure 3.--Vertical cross-section of radiosonde temperature observations (°C) on Apr. 6, 1973, at 0000 GMT

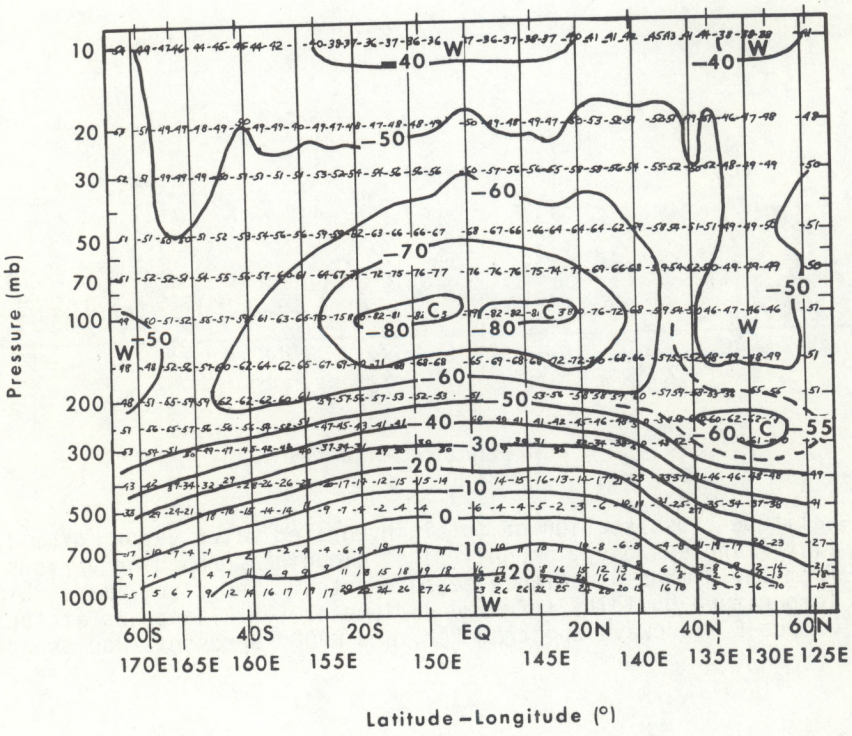

Figure 4.--Vertical cross-section of Nimbus-5 temperature observations (°C) on Apr. 6, 1973, at 0121 to 0204 GMT

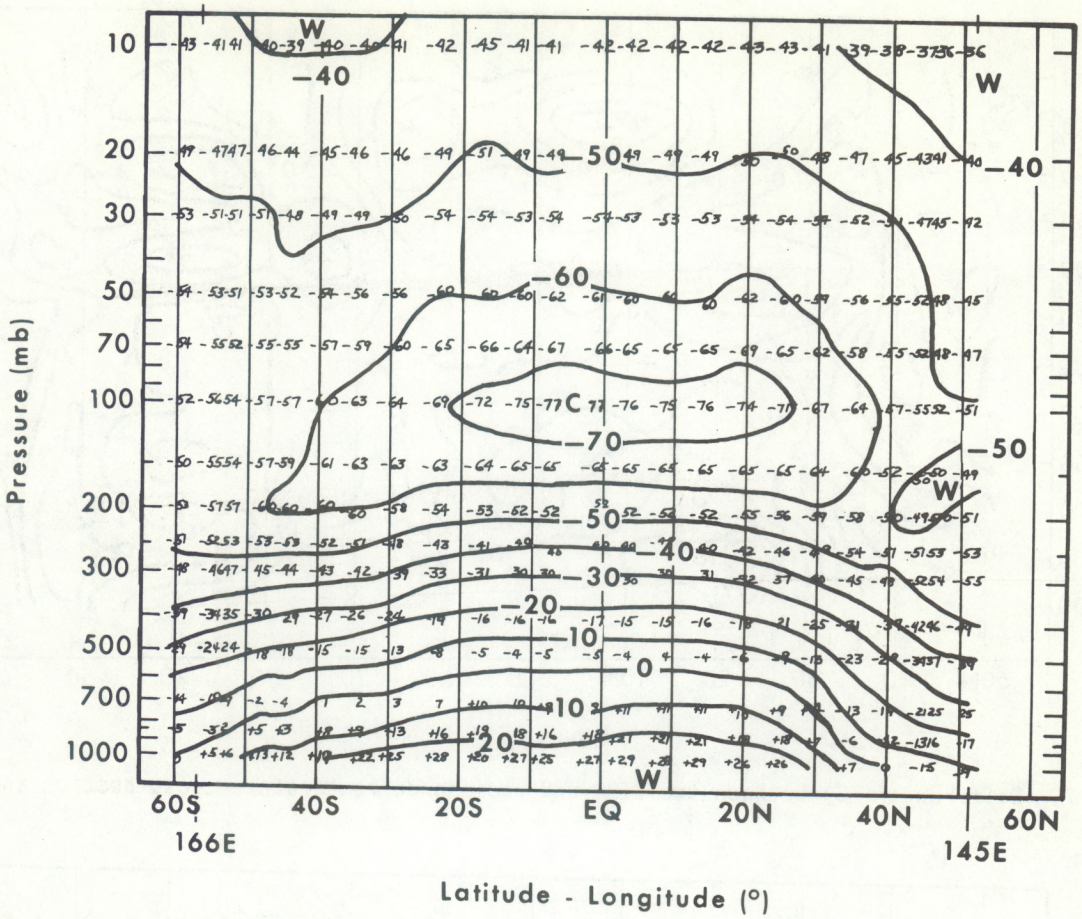

Figure 5.--Vertical cross-section of NOAA-2 VTPR temperature observations (°C) on Apr. 5, 1973, at 2023 to 2355 GMT

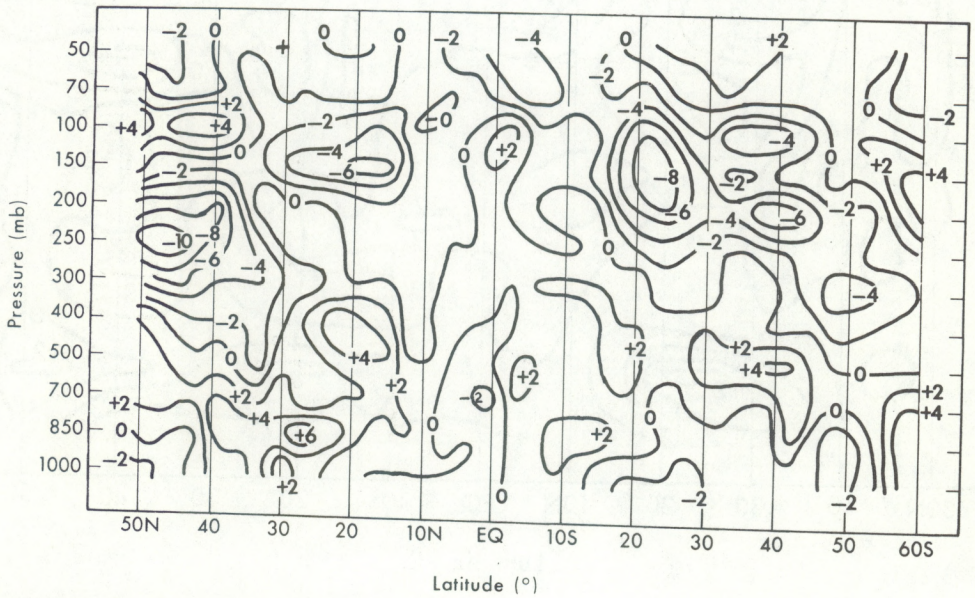

Figure 6.--Difference (°C) between the Nimbus-5 and radiosonde temperature cross-section analyses

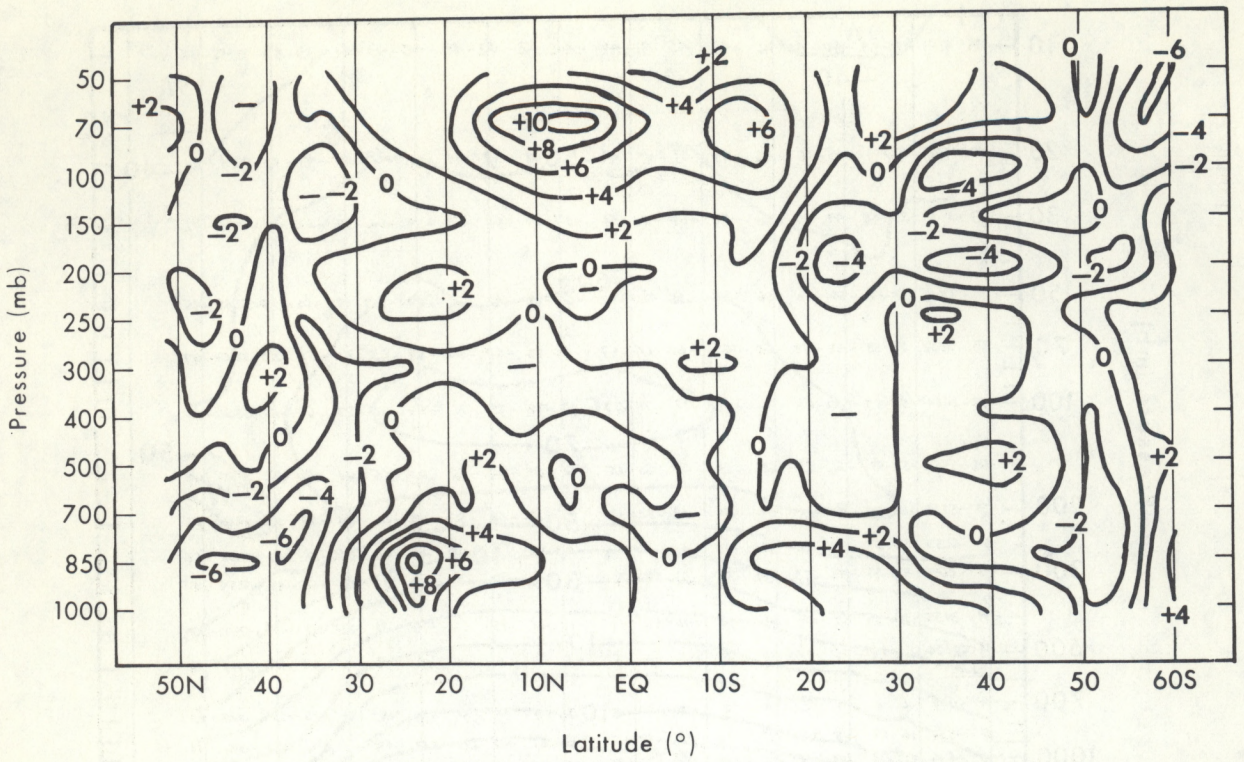

Figure 7.--Difference (°C) between the VTPR and radiosonde temperature cross-section analyses

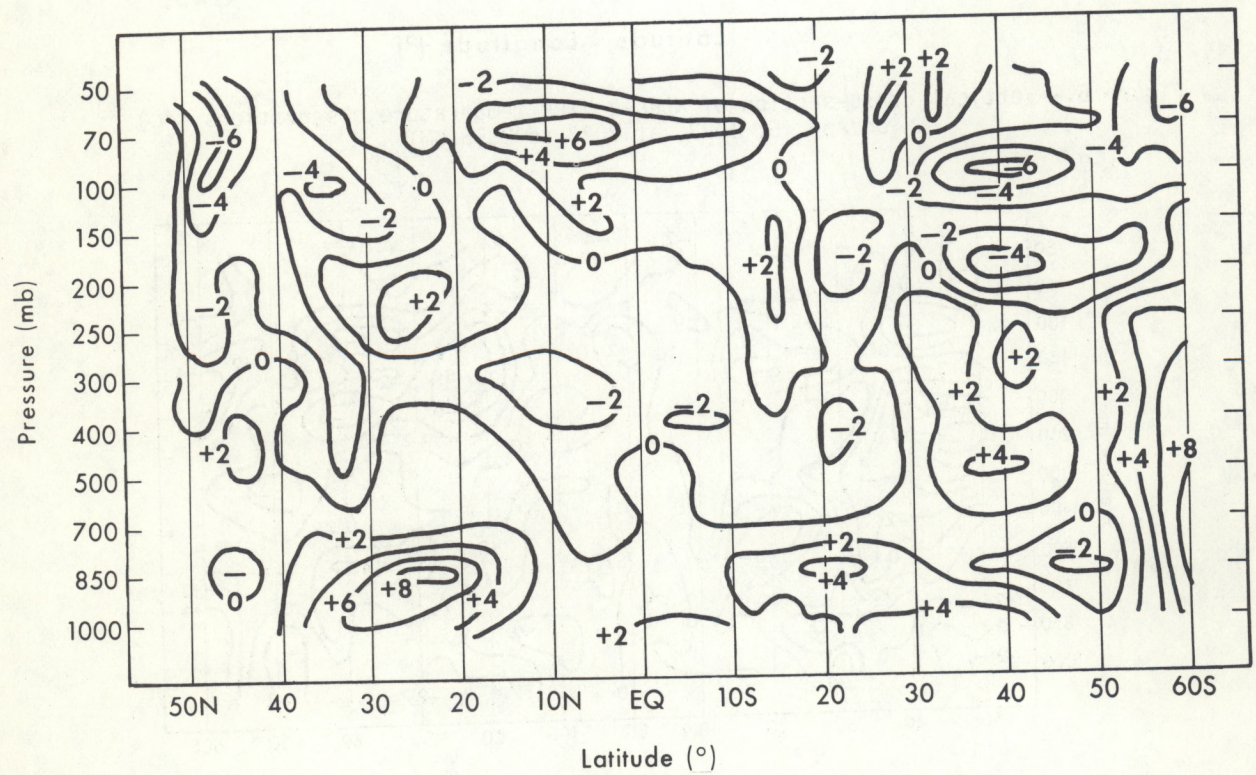

Figure 8.--Difference (°C) between the 12-hr forecast and radiosonde temperature cross-section analyses

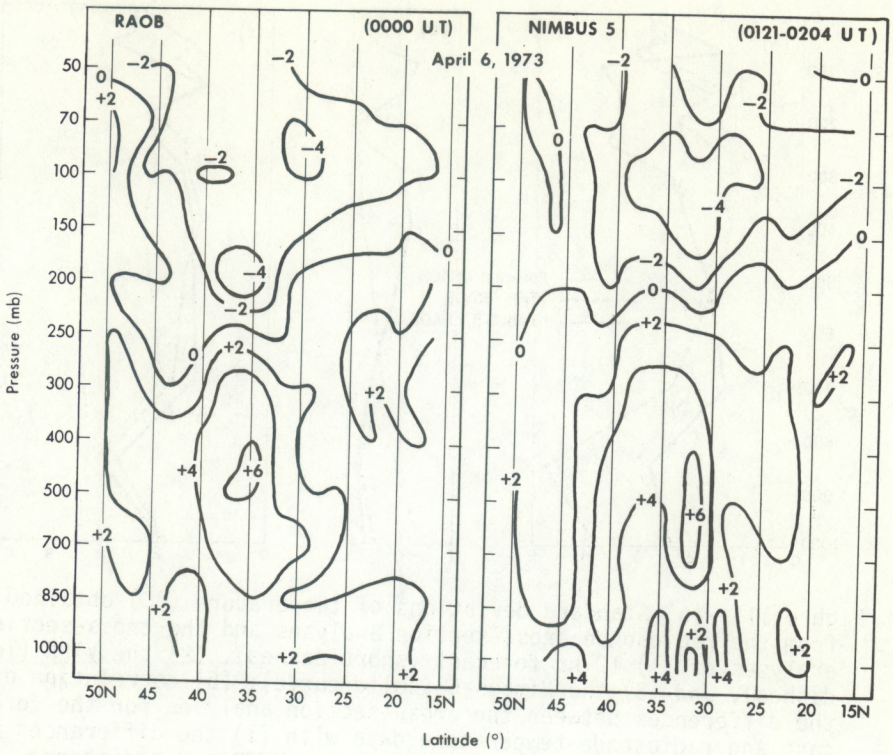

Figure 9.--Radiosonde and Nimbus-5 temperature gradients over 3° latitude obtained from the cross-section analyses

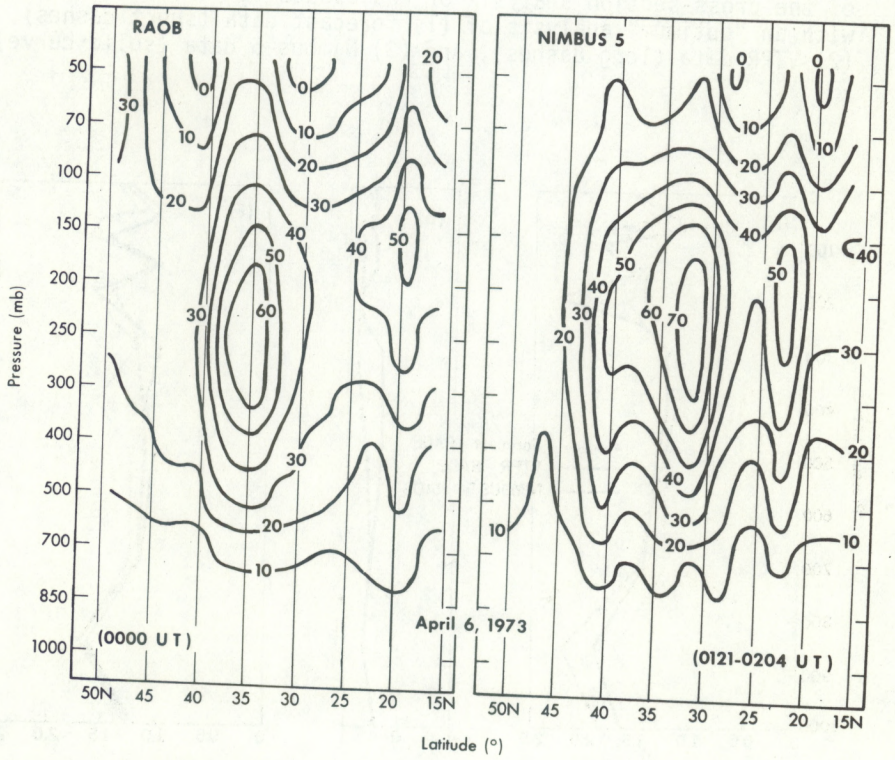

Figure 10.--Geostrophic (integrated thermal) winds (m/s) computed from the radiosonde and Nimbus-5 temperature cross-sections

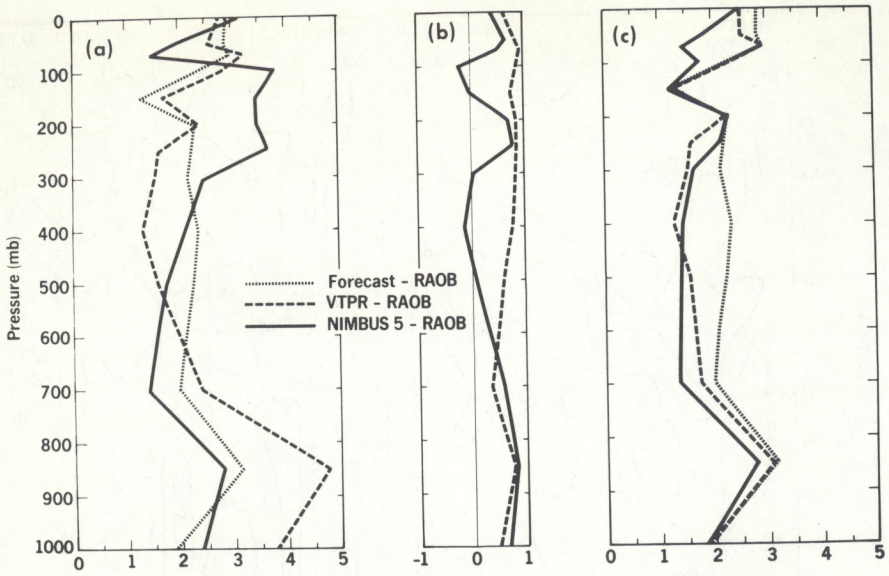

Figure 11.--(a) Standard deviations of temperature (°C) obtained from the radiosonde cross-section analyses and the cross-section analyses of (1) 12-hr forecast (short dashes), (2) the VTPR (long dashes), and (3) the Nimbus-5 (solid curve); (b) correlation of the differences between the cross-section analyses for the forecast and radiosonde temperature data with (1) the differences between the cross-section analyses for the VTPR and radiosonde temperature data (dashed curve) and (2) the differences between the cross-section analyses for the Nimbus-5 and radiosonde temperature data (solid curve); and (c) expected standard deviations of the cross-section analysis of radiosonde temperature data with an "optimum" analysis of (1) forecast data (short dashes), (2) VTPR data (long dashes), and (3) Nimbus-5 data (solid curve)

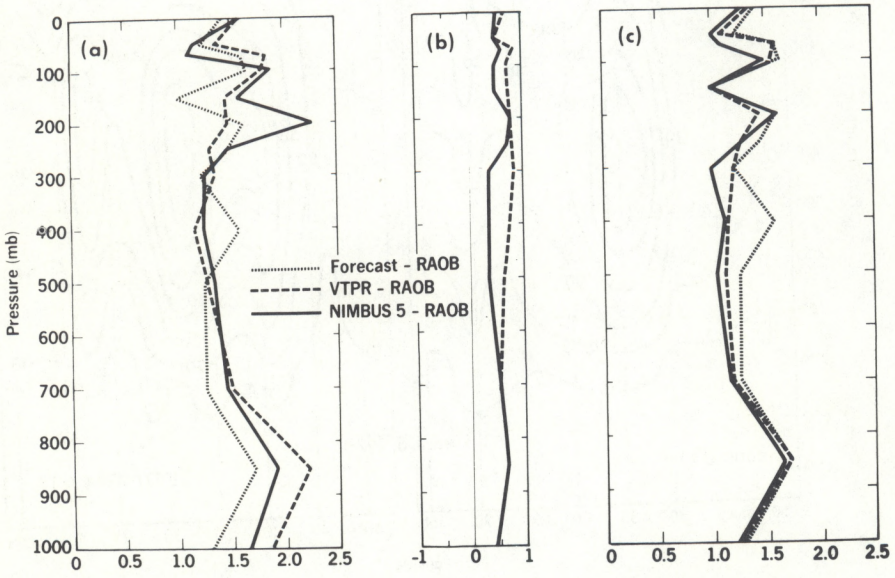

Figure 12.--Same as figure 11 except here it is for temperature gradients (°C) over 3° of latitude

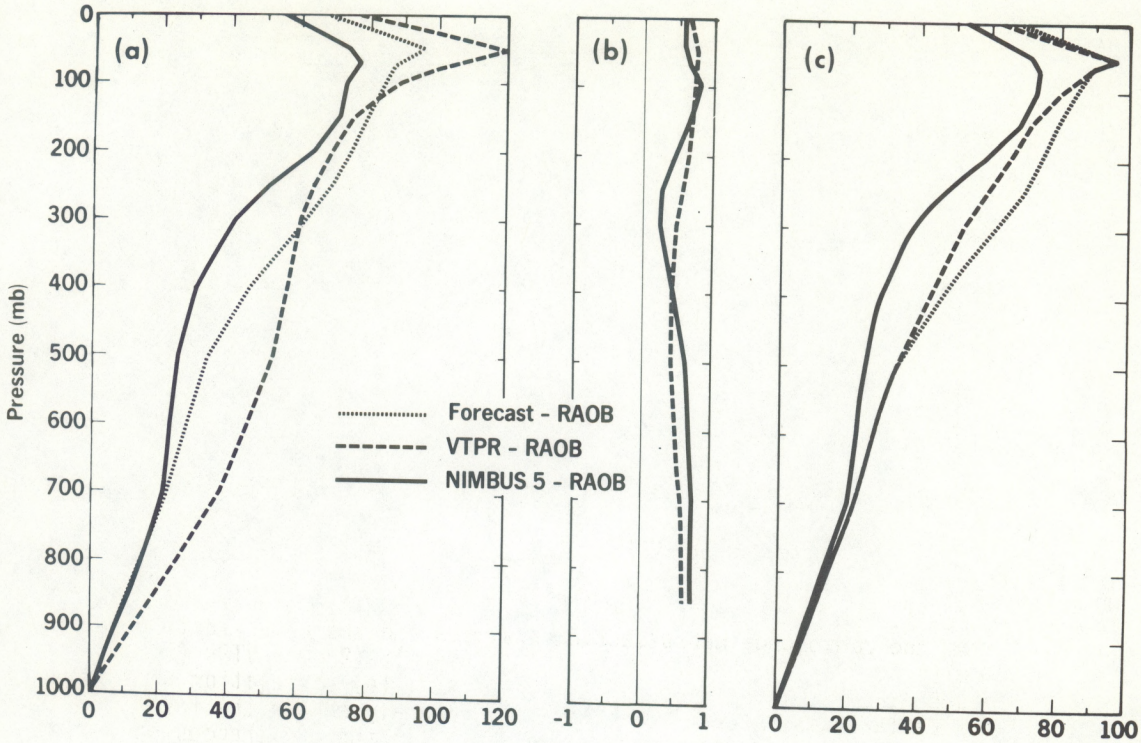

Figure 13.--Same as figure 11 except here it is for geopotential height (m)

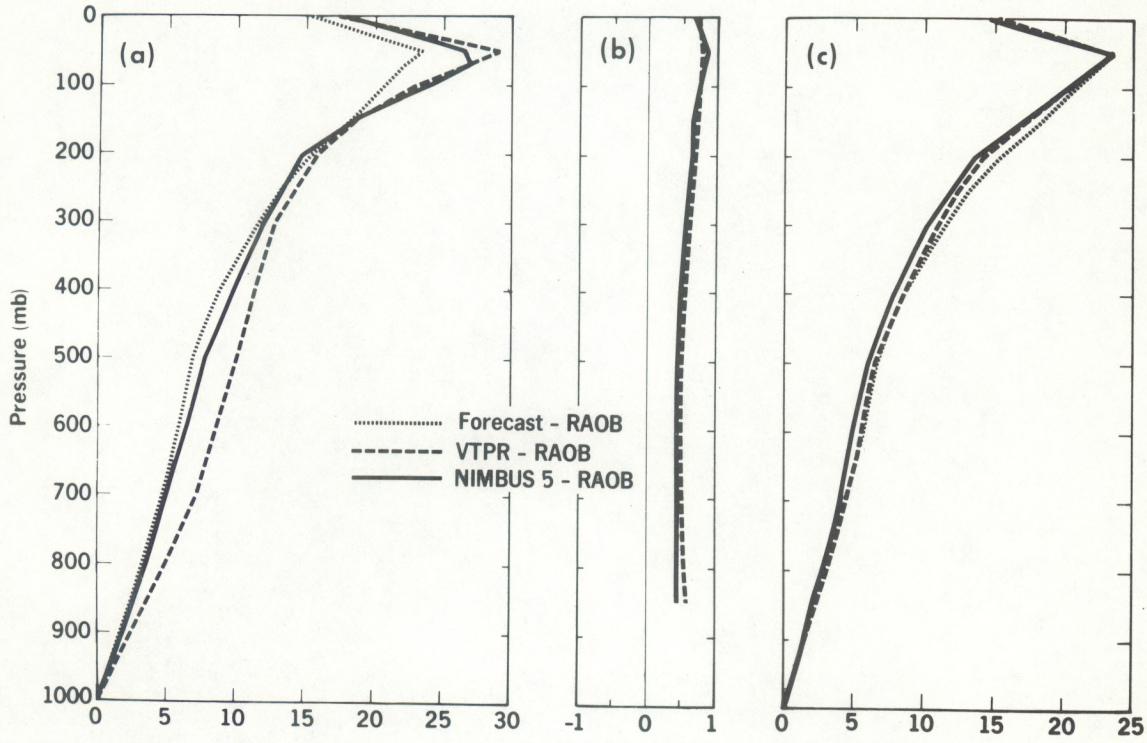

Figure 14.--Same as figure 11 except here it is for geostrophic wind (m/s)

(Continued from inside front cover)

NESC 51 Application of Meteorological Satellite Data in Analysis and Forecasting. Ralph K. Anderson, Jerome P. Ashman, Fred Bittner, Golden R. Farr, Edward W. Ferguson, Vincent J. Oliver, and Arthur H. Smith, September 1969 (AD-697-033). Supplement (AD-740-017).

NESC 52 Data Reduction Processes for Spinning Flat-Plate Satellite-Borne Radiometers. Torrence H. MacDonald, July 1970. (COM-71-00132)

NESC 53 Archiving and Climatological Applications of Meteorological Satellite Data. John A. Leese, Arthur L. Booth, and Frederick A. Godshall, July 1970. (COM-71-00076)

NESC 54 Estimating Cloud Amount and Height From Satellite Infrared Radiation Data. P. Krishna Rao, July 1970. (PB-194-685)

NESC 56 Time-Longitude Sections of Tropical Cloudiness (December 1966-November 1967). J. M. Wallace, July 1970. (COM-71-00131)

NOAA Technical Reports

NESS 55 The Use of Satellite-Observed Cloud Patterns in Northern Hemisphere 500-mb Numerical Analysis. Roland E. Nagle and Christopher M. Hayden, April 1971. (COM-73-50262)

NESS 57 Table of Scattering Function of Infrared Radiation for Water Clouds. Giichi Yamamoto, Masayuki Tanaka, and Shoji Asano, April 1971. (COM-71-50312)

NESS 58 The Airborne ITPR Brassboard Experiment. W. L. Smith, D. T. Hilleary, E. C. Baldwin, W. Jacob, H. Jacobowitz, G. Nelson, S. Soules, and D. Q. Wark, March 1972. (COM-72-10557)

NESS 59 Temperature Sounding From Satellites. S. Fritz, D. Q. Wark, H. E. Fleming, W. L. Smith, H. Jacobowitz, D. T. Hilleary, and J. C. Alishouse, July 1972. (COM-72-50963)

NESS 60 Satellite Measurements of Aerosol Backscattered Radiation From the Nimbus F Earth Radiation Experiment. H. Jacobowitz, W. L. Smith, and A. J. Drummond, August 1972. (COM-72-51031)

NESS 61 The Measurement of Atmospheric Transmittance From Sun and Sky With an Infrared Vertical Sounder. W. L. Smith and H. B. Howell, September 1972. (COM-73-50020)

NESS 62 Proposed Calibration Target for the Visible Channel of a Satellite Radiometer. K. L. Coulson and H. Jacobowitz, October 1972. (COM-73-10143)

NESS 63 Verification of Operational SIRS B Temperature Retrievals. Harold J. Brodrick and Christopher M. Hayden, December 1972. (COM-73-50279)

NESS 64 Radiometric Techniques for Observing the Atmosphere From Aircraft. William L. Smith and Warren J. Jacob. January 1973. (COM-73-50376)

NESS 65 Satellite Infrared Soundings From NOAA Spacecraft. L. M. McMillin, D. Q. Wark, J.M. Siomkajlo, P. G. Abel, A. Werbowetzki, L. A. Lauritson, J. A. Pritchard, D. S. Crosby, H. M. Woolf, R. C. Luebbe, M. P. Weinreb, H. E. Fleming, F. E. Bittner, and C. M. Hayden, September 1973. (COM-73-50936/6AS)

NESS 66 Effects of Aerosols on the Determination of the Temperature of the Earth's Surface From Radiance Measurements at 11.2 μm. H. Jacobowitz and K. L. Coulson, September 1973. (COM-74-50013)

NESS 67 Vertical Resolution of Temperature Profiles for High Resolution Infrared Radiation Sounder (HIRS). Y. M. Chen, H. M. Woolf, and W. L. Smith, January 1974. (COM-74-50230)

NESS 68 Dependence of Antenna Temperature on the Polarization of Emitted Radiation for a Scanning Microwave Radiometer. Norman C. Grody, January 1974. (COM-74-50431/AS)

NESS 69 An Evaluation of May 1971 Satellite-Derived Sea Surface Temperatures for the Southern Hemisphere. P. Krishna Rao, April 1974. (COM-74-50643/AS)

NESS 70 Compatibility of Low-Cloud Vectors and Rawins for Synoptic Scale Analysis. L. F. Hubert and L. F. Whitney, Jr., October 1974.